Corolla Is a Novel Protein That Contributes to the Architecture of the Synaptonemal Complex of *Drosophila*

Kimberly A. Collins,*,[1] Jay R. Unruh,* Brian D. Slaughter,* Zulin Yu,* Cathleen M. Lake,* Rachel J. Nielsen,* Kimberly S. Box,*,[2] Danny E. Miller,*,[†] Justin P. Blumenstiel,[‡] Anoja G. Perera,* Kathryn E. Malanowski,* and R. Scott Hawley*,[†,3]

*Stowers Institute for Medical Research, Kansas City, Missouri 64110, [‡]Department of Ecology and Evolutionary Biology, University of Kansas, Lawrence, Kansas 66045, and [†]Department of Molecular and Integrative Physiology, University of Kansas Medical Center, Kansas City, Kansas 66160

ABSTRACT In most organisms the synaptonemal complex (SC) connects paired homologs along their entire length during much of meiotic prophase. To better understand the structure of the SC, we aim to identify its components and to determine how each of these components contributes to SC function. Here, we report the identification of a novel SC component in *Drosophila melanogaster* female oocytes, which we have named Corolla. Using structured illumination microscopy, we demonstrate that Corolla is a component of the central region of the SC. Consistent with its localization, we show by yeast two-hybrid analysis that Corolla strongly interacts with Cona, a central element protein, demonstrating the first direct interaction between two inner-synaptonemal complex proteins in *Drosophila*. These observations help provide a more complete model of SC structure and function in *Drosophila* females.

THE Laws of Mendelian Inheritance are little more than a statistical restatement of the events that underlie the proper segregation of homologous chromosomes at the first meiotic division. Homologous segregation requires a number of distinct processes, such as pairing and recombination, but our focus here is on the formation of a complex, proteinaceous structure known as the synaptonemal complex (SC). The SC forms between homologous chromosomes during early meiotic prophase and is essential for such functions as the maintenance of homolog pairing, the conversion of programmed double-strand breaks (DSBs) into crossovers (Page and Hawley 2004), and the facilitation of both homologous and heterologous centromeric associations (Takeo *et al.* 2011; Tanneti *et al.* 2011).

In terms of its overall structure and dimensions, the SC is highly conserved (Carpenter 1975; Zickler and Kleckner 1999; Schild-Prüfert *et al.* 2011; Fraune *et al.* 2012a), consisting of two lateral elements (LEs) and a central region (CR). The CR is composed of both transverse filament (TF) proteins and central element (CE) proteins. LE proteins run the length of each homolog and function to connect the sister chromatids and to compact the chromosome axes with a complex composed of cohesins as well as SC-specific components (Lammers *et al.* 1994; Anderson *et al.* 2005; Khetani and Bickel 2007; Alsheimer *et al.* 2010; Watts and Hoffmann 2011). In *Drosophila melanogaster*, the SC-specific components of the LE are Ord, Solo, and C(2)M (Manheim and McKim 2003; Webber *et al.* 2004; Anderson *et al.* 2005; Khetani and Bickel 2007; Yan and McKee 2013). The CE is located at the very center of the SC. In *Drosophila*, the protein Cona is thought to be a component of the CE. Cona appears to be required for "zippering" together the TF proteins that both span the width of the SC and overlap in an interlocking manner at the center of the SC (Page *et al.* 2008). Many organisms appear to have a single TF protein; however, *Caenorhabditis elegans* has multiple TF proteins that

doi: 10.1534/genetics.114.165290
Manuscript received April 14, 2014; accepted for publication May 29, 2014; published Early Online June 9, 2014.
Available freely online through the author-supported open access option.
Supporting information is available online at http://www.genetics.org/lookup/suppl/doi:10.1534/genetics.114.165290/-/DC1.
[1]Present address: Department of Comparative Medicine, University of Washington, Seattle, WA 98109.
[2]Present address: Department of Molecular Biology, Princeton University, Princeton, NJ 08544.
[3]Corresponding author: Stowers Institute for Medical Research, Kansas City, MO 64110. E-mail: rsh@stowers.org

act together to bridge the width of the SC (MacQueen *et al.* 2002; Colaiácovo *et al.* 2003; Smolikov *et al.* 2007, 2009; Schild-Prüfert *et al.* 2011).

Although it has long been thought that *Drosophila* also possesses a single TF protein, known as C(3)G (Page and Hawley 2001), we will present evidence below that the novel protein Corolla is a TF protein. Corolla is encoded by a novel *Drosophila* gene, *CG8316*, and *corolla* mutants are defective in SC assembly and/or maintenance. Using structured illumination microscopy (SIM), we show that Corolla localizes to the CR of the *Drosophila* SC. Consistent with Corolla's localization to the CR by SIM, we show that Corolla physically interacts with Cona, demonstrating the first direct interaction between two inner-SC proteins in *Drosophila*. We propose that Corolla, which possesses several predicted coiled-coil domains, functions both by directly binding to Cona and by interacting with C(3)G, perhaps via the coiled-coil domains of C(3)G and Corolla, to stabilize the ability of C(3)G to link the LEs to the CE and thereby establish the SC.

Materials and Methods

Drosophila genetics

All stocks were maintained on standard medium containing yeast, cornmeal, corn syrup, malt extract, and agar at 25°, and include *y w cv v corolla^{1} FRT19A/C(1)DX*, *y f/Y* (Collins *et al.* 2012), *y w corolla^{1} FRT19A/C(1)DX*, *y f/y^{+}Y* (Collins *et al.* 2012), *w^{1118} P{XP}CG8316^{d01774}/C(1)DX*, *y f/y^{+}Y* (created from stock Bloomington 19165), and *Df(1)BSC643* (Bloomington 25733), *w^{1118}/Binsinscy*, *Df(1)BSC583*, and *w^{1118}/Binsinscy* (Bloomington 25417) were used in mapping *corolla*. *w*; *pCa4-attB-genomic-Corolla* (this study), *okra^{AA} cn bw/CyO* (Ghabrial *et al.* 1998), *okra^{RU} cn bw*/CyO (Ghabrial *et al.* 1998), *ru^{1} h^{1} th^{1} st^{1} cu^{1} sr^{1} e^{s} ca^{1}* (Bloomington 576), *ru^{1} h^{1} th^{1} st^{1} cu^{1} sr^{1} e^{s} Pr^{1} ca/TM6B*, *Bri^{1} Tb^{1}* (Bloomington 1711), and *ru^{1} h^{1} th^{1} st^{1} cu^{1} sr^{1} e^{s} ca^{1}/TM3, Sb* were used in recombination assays. Other stocks used: *nanos-Gal4*; *cona^{f04903}/TM3, y w eyFLP*; *FRT82B y^{+} TPN1*, *Tb Ser* (Page *et al.* 2008), *yw eyFLP;FRT82B cona^{A12}/TM6B y^{+} TPN1*, *Tb* (Page *et al.* 2007), *y w FRT19A/hs-hidY* (used as wild-type stock) (Collins *et al.* 2012), *y w nanos-Gal4/FM7a*; *c(3)G^{68}e ca/TM3, Ser* (Jeffress *et al.* 2007), *y w* ; *P{UASP}-c(3)G$^{Cdel4\text{-}Flag}$* ; *c(3)G$^{[68]}$ e/TM3, Sb Ser e*; *spa^{pol}/+* (Jeffress *et al.* 2007), and *w/B^{s}Y*; *c(3)G^{68}e/TM3, Ser*.

The following genotypes were used throughout and represent the null genotypes of *corolla*, *cona*, *c(3)G*, and *okra*: *y w cv v corolla^{1} FRT19A/y w corolla^{1} FRT19A*, *cona^{f04903}/cona^{A12}*, *c(3)G^{68} e/c(3)G^{68} e ca* and *okra^{AA} cn bw/okra^{RU} cn bw*, respectively.

To assay chromosome nondisjunction, tester female virgins were crossed to *X^Y*, *In(1)EN,v f B*; *C(4)RM,ci ey^{R}* males. Calculations were performed as previously described (Zitron and Hawley 1989; Hawley *et al.* 1992). To assay recombination on the third chromosome, single tester female virgins (either *y w FRT19A*; *ru h th st cu sr e^{s} Pr ca/+* or *y w corolla FRT19A*; *ru h th st cu sr e^{s} Pr ca/+*) were crossed to *ru h th st cu sr e^{s} ca* males in vials and all single and double recombinants in the female progeny between *th* and *ca* were scored through day 18.

Mapping of the corolla mutants to CG8316

Next-generation sequencing (NGS) was used to identify the causative lesion in the novel complementation group previously reported (Collins *et al.* 2012), which contains mutants *corolla^{1}*, *corolla^{129}*, and *corolla^{166}*. A multi-allele whole-genome sequencing approach was done for two of these alleles (*corolla^{1}* and *corolla^{129}*) and compared to the parental stock used in the screen, *y w FRT19A*, according to Blumenstiel *et al.* (2009) with the following modifications.

For each NGS sample, 1–3 μg of genomic DNA was sheared to <700-bp fragments using a Bioruptor sonicator (Diagenode). Following the manufacturer's directions, short fragment libraries were made using the Illumina TruSeq DNA LT Sample Prep Kit v2-set B (Illumina, catalog no. FC-121-2002). The resulting libraries were quantified using a Bioanalyzer (Agilent Technologies) and a Qubit Fluorometer (Life Technologies). All libraries were pooled, quantified, and run as 100-bp paired-end reads on an Illumina HiSequation 2000 instrument using HiSeq Control Software 1.4.8. Following sequencing, Illumina Primary Analysis version RTA 1.12.4.2 and Secondary Analysis version CASAVA-1.8.2 were run to demultiplex reads and generate FASTQ files.

Reads were trimmed to 90 bp by the FastX toolkit (http://hannonlab.cshl.edu/fastx_toolkit/index.html). Reads were aligned to the University of California at Santa Cruz dm3 reference genome using BWA, version 0.5.9 (Li and Durbin 2009). Duplicate reads potentially caused by amplification were removed using samtools rmdup. Samtools and Picard were used to index and sort the reads to prepare for variant analysis. Aligned data is available at NCBI under accession numbers 2899034, 2899035, and 2899036.

Indel and SNP detection was performed using the GATK pipeline (McKenna *et al.* 2010; DePristo *et al.* 2011). This tool was used to perform local realignment around indels and then call SNPs and indels for the region of interest. Predicted variant effects were found using the snpEff tool (version 2.0.5d) (Cingolani *et al.* 2012). Post processing, filtering, and analysis of variants was performed using custom scripts.

Three SNPs were detected within the *CG8316* gene region in the parental stock compared with the reference sequence. The "extended gene region" of *CG8316* from FlyBase (release 5.43) was downloaded; the first nucleotide is equivalent to position 1 in the following SNP designations. The three SNPs correspond to the synonymous mutation *G2299A* in exon 2; *G3776T* in exon 4, which results in an Asp-to-Glu amino acid change; and a deletion of *4067A* after the stop codon in exon 4.

corolla^{1} has an *A2759T* mutation in *CG8316*, resulting in a single stop codon at amino acid 173; *corolla^{129}* has a 23-bp deletion located at position 2814–2836 (just 1 bp following

amino acid 190), which results in a frameshift leading to a series of stop codons with the first beginning at amino acid 199; and *corolla*^{166} has a *C2804T* mutation, which creates a single stop codon at amino acid 188 (Figure 1A). *CG8316* was the only gene on the *X* chromosome that we identified that had a single nucleotide polymorphism or a deletion in the two mutant chromosomes tested when compared to the reference parental chromosome.

Transgene rescue

For transgene rescue of *corolla*, a genomic rescue construct was made by performing PCR on the *y w FRT19A* stock that was used for the mutagenesis in which *corolla* was isolated. The transgene included 1019 bp upstream of the start codon of *CG8316* and 227 bp of downstream sequence, which includes the 3′ untranslated region. Naturally occurring *Spe*I and *Bam*HI sites were utilized for cloning this genomic fragment. The entire gene region was sequenced after cloning into *pCaspeR4-attB* (gift from the Perrimon laboratory) at *Spe*I and *Bam*HI sites in the multi-cloning region for site-specific integration at *attP40* (Genetic Services) (Markstein *et al.* 2008).

Yeast two-hybrid

The Matchmaker Gold Yeast Two-Hybrid System User Manual (Clontech Protocol no. PT4084-1, Version No. PR033493) was followed for yeast transformation, testing for autoactivation, and for yeast two-hybrid assays. AH109 yeast were used in place of Y2Hgold. The AH109 genotype is as follows: *MATα*, *trp1-901*, *leu2-3*, *112*, *ura3-52*, *his3-200*, *gal4Δ*, *gal80Δ*,*LYS2*:: $GAL1_{UAS}$-$GAL1_{TATA}$-*HIS3*, $GAL2_{UAS}$-$GAL2_{TATA}$-*ADE2*, *URA3*:: $MEL1_{UAS}$-$MEL1_{TATA}$-*lacZ* (James *et al.* 1996). The Y187 genotype is as follows: *MATα*, *ura3-52*, *his3-200*, *ade2-101*, *trp1-901*, *leu2-3*, *112*, *gal4Δ*, *met–*, *gal80Δ*, *URA3*:: $GAL1_{UAS}$-$GAL1_{TATA}$-*lacZ* (Wade Harper *et al.* 1993). BD-Corolla autoactivated the *HIS3* reporter but did not autoactivate the *ADE2* reporter and only weakly autoactivated the *MEL1* reporter (data not shown).

Cytology

Germarium preparations for whole-mount immunofluorescence were as according to Page and Hawley (2001) with minor exceptions. Females (0- to 1-day-old) were collected and yeasted overnight in the presence of males. Ovaries were dissected in PBS for no longer than 20 min prior to fixing. In all incubation steps, ovaries were incubated at room temperature while nutating unless otherwise specified. Ovaries were then washed three times for 10 min in PBS with 0.1% Tween (PBST). Ovaries were cut at approximately stage 4–5, and the tips containing the germarium were dissected apart with forceps. Germarium tips were then blocked in PBST with 1% BSA for 1 hr, and the primary antibody diluted in PBST was incubated with germarium tips overnight at 4° while nutating. After washing three times for 15 min in PBST, the secondary antibodies were applied for 4 hr followed by the addition of 4′6-diamididino-2-phenylindole at a concentration of 1 μg/ml for the final 10 min of incubation. After washing as before, the samples were mounted in ProLong Gold (Invitrogen) and allowed to cure for 24 hr. Chromosome spreads were prepared as described in Khetani and Bickel (2007) with the two following minor exceptions: 16% formaldehyde (Ted Pella) was diluted to 1% in water and pH was not adjusted. Normal goat serum was substituted for normal donkey serum in the blocking solution.

Mouse anti-C(3)G 1A8-1G2 was used at 1:500 (Anderson *et al.* 2005). Rabbit anti-Corolla (animal 210) was used at 1:1000 or 1:1500 in all experiments with indistinguishable results (this study). Guinea pig anti-Cona was used at 1:500 (Page *et al.* 2008). Rat anti-CID (gift of Sunkel laboratory) was used at 1:1000 (Martins *et al.* 2009). Guinea pig anti-SMC1 was used at 1:500 (Khetani and Bickel 2007). Mouse anti-Orb antibodies 4H8 and 6H4 (Developmental Studies Hybridoma Bank) were used at 1:50 each. Anti-Flag M2 antibody (Sigma) was used at 1:500. Mouse anti-γ-H2AV (Lake *et al.* 2013) supernatant was used at 1:500. In experiments where both mouse anti-γ-H2AV (isotype IgG2b-kappa) and mouse anti-Orb were used together, only anti-Orb 4H8 (isotype IgG1) was used. Secondary goat anti-mouse, rabbit, guinea pig, or rat Alexa-488, Alexa-555, and Alexa-647 IgG heavy and light chain or isotype-specific (IgG1 and IgG2b) conjugated antibodies were used at 1:500 (Molecular Probes).

With the exception of Figure 2 and Figure S2, all images were acquired with a DeltaVision microscopy system (GE Healthcare) consisting of a 1 × 70 inverted microscope with a high-resolution CCD camera. Images were deconvolved using SoftWoRx (Applied Precision/GE Healthcare) software, and maximum intensity projections were made unless otherwise noted.

SIM images were acquired on an Applied Precision OMX Blaze microscope (GE Healthcare) equipped with a PCO Edge sCMOS camera (Kelheim, Germany). An Olympus (Center Valley, PA) 60× 1.42 numerical aperture Plan Apo N oil objective was used. SIM reconstruction was performed with the Applied Precision Softworx software package (GE Healthcare, Piscataway, NJ) following the Applied Precision protocols. All analysis was performed using ImageJ and custom plugins written for ImageJ available at http://research.stowers.org/imagejplugins. Prior to analysis, the SIM reconstructed image was scaled 2 by 2 with bilinear interpolation. Alignment between differently colored channels was performed on single slices or projections using the TurboReg plugin for ImageJ (Thevenaz *et al.* 1998). Well-formed regions of the SC that ran approximately parallel to the *xy* plane were manually selected, and intensity profiles were averaged over a three-pixel-wide stripe perpendicular to the SC. For C(3)G distance measurements, these intensity profiles were then fit to double Gaussian functions with a background component.

Sanger sequencing

DNA was isolated from a single aged male according to Gloor *et al.* (1993). Sequencing primers for *CG8316/corolla* are available upon request.

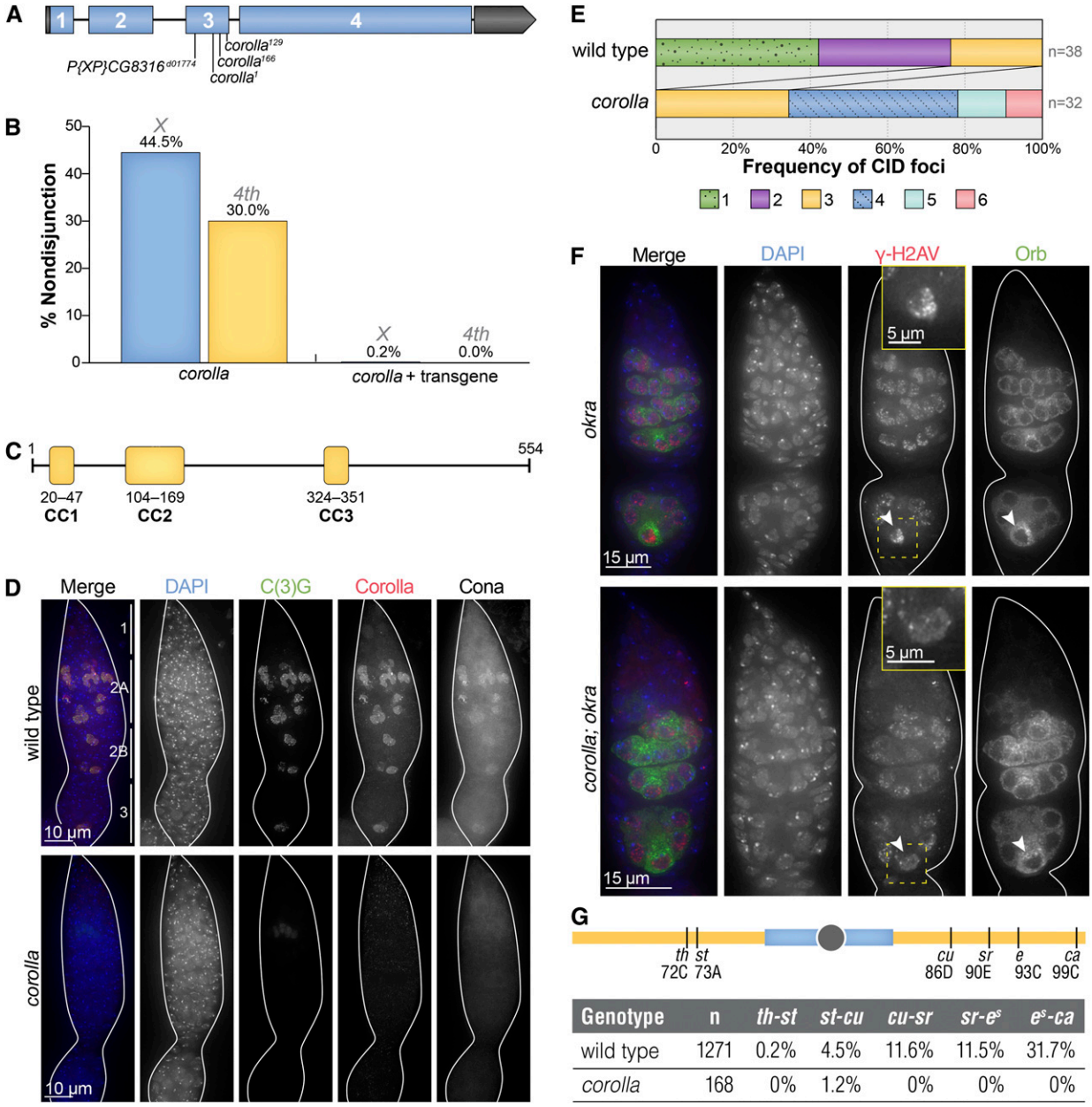

Genotype	n	*th-st*	*st-cu*	*cu-sr*	*sr-e*^{s}	*e*^{s}*-ca*
wild type	1271	0.2%	4.5%	11.6%	11.5%	31.7%
corolla	168	0%	1.2%	0%	0%	0%

Figure 1 Corolla is an essential component of the *Drosophila* SC. (A) A schematic of the *CG8316* gene region shows the relative location of the *corolla* alleles with coding sequence in blue and the 5′ and 3′ untranslated regions in gray. Note that all alleles are located in exon 3. Mutations in *corolla*^{1}, *corolla*^{129}, and *corolla*^{166} are predicted to truncate the protein at amino acids 173, 199, and 188, respectively (see *Materials and Methods*). (B) *corolla* exhibits elevated levels of *X* and *4*th chromosome nondisjunction, which can be fully suppressed by expression of one copy of *corolla* (*pCa4-genomic-Corolla-attB*). (C) A schematic of Corolla showing the location of the internal coiled-coil domains as predicted by Coils (http://embnet.vital-it.ch/software/COILS_form.html). (D) Immunofluorescence of wild-type and *corolla* mutant germaria showing that in wild type Corolla (red in merge) localizes exclusively to the SC in oocytes throughout pachytene, as demonstrated by the colocalization of C(3)G (green in merge) and Cona; however, in the absence of *corolla*, no SC can be detected. (E) *corolla* mutants are defective in centromere clustering, displaying an average of 3.97 ± 0.93 CID foci compared to 1.80 ± 0.80 CID foci in wild type. The number of oocyte nuclei scored from region 3 of the germarium, identified by Orb staining, is shown at the right of the graph. (F) Immunofluorescence analysis showing that the number of DSBs formed in the *corolla* mutant is reduced when examined in the background of the DSB-repair-deficient mutant *okra*. Arrowheads identify the oocyte nuclei in region 3 of the germarium with concentrated Orb staining and accumulated DSBs. See Table S2 for γ-H2AV region 3 foci counts. For each genotype, the oocyte nucleus is shown at higher magnification within the γ-H2AV panel in the inset. (G) *corolla* mutants are defective in meiotic recombination as assayed on the *3*rd chromosome. Euchromatin is indicated by yellow and heterochromatin by blue. The frequency of recombination is shown for the five intervals examined.

Centromere clustering analysis

Analysis was performed as previously described (Takeo *et al.* 2011). We analyzed oocyte nuclei in region 3 of the germarium in both wild-type and SC-defective lines. Region 3 oocytes were identified by costaining with the cytoplasmic marker Orb.

Generation of polyclonal anti-Corolla antibodies

The cDNA of *CG8316* (Berkeley *Drosophila* Genome Project, *Drosophila* Gene Collection #LD15362) was amplified with primers containing *Nde*I and *Bam*HI sites (primer sequence available upon request) and subcloned into *pET19b* at *Nde*I and *Bam*HI sites within the multi-cloning region. The clone was sequence-verified and transformed into BL21 DE3 cells (New England Biolabs). Protein expression was done following the QiaExpressionist Handbook for purification under denaturing conditions, and the 6xHis protein was purified using ProBond Nickel Chelating Resin (Invitrogen). Antibodies were made in rabbits using 6xHis-Corolla protein as antigen (Cocalico Biologicals, Inc). Pre-immune rabbit (animal 210) serum did not stain *Drosophila* ovaries (data not shown).

Quantification of γ-H2AV foci

To score the number of γ-H2AV foci, we first identified the nuclei of the oocyte in region 3 cysts that had concentrated cytoplasmic Orb staining. *okra* mutants also display a delay in selection of the oocyte (Joyce and McKim 2009). Therefore, in those region 3 cysts that had two oocytes, both oocytes were scored as if each had concentrated Orb staining and robust SC staining. We then identified the z-stacks pertaining to the oocyte nuclei. Using Imaris 7.0.0 software (Bitplane, Zurich, Switzerland), we performed a 3D crop of the selected nuclei and displayed the z-sections using the gallery function. Only clearly defined foci where counted in the corresponding z-series.

Results

The *corolla* gene was first identified by the recovery of three allelic mutants, originally named *mei-39*^{1}, *mei-39*^{129}, and *mei-39*^{166}, in a screen for *X*-linked meiotic mutants in *Drosophila* (Collins *et al.* 2012). Based on the cytological phenotype that we will describe below, we have named this gene *corolla*. We also have renamed the *mei-39*^{1}, *mei-39*^{129}, and *mei-39*^{166} mutants *corolla*^{1}, *corolla*^{129}, and *corolla*^{166}.

As described in *Materials and Methods*, these mutants were mapped by whole-genome sequencing to a transcription unit denoted *CG8316* (Figure 1A). The meiotic phenotype exhibited by these *corolla* alleles was confirmed to be the result of mutations in *CG8316* by showing that two overlapping deficiencies that uncover *CG8316* and a *P*-element insertion mutation, *P{XP}CG8316*^{d01774}, fail to complement the *corolla*^{1} allele as assayed by measuring meiotic nondisjunction (data not shown). We further showed by a transgene rescue assay that expression of *CG8316* fully suppresses the meiotic nondisjunction phenotype of the *corolla*^{1} mutant (Figure 1B).

Table 1 Comparison of fertility of wild type, *corolla*, and *corolla* with the rescue construct

Genotype	*n*[a]	Total progeny	Average per vial	% of wild type
Wild type	8	402	50.3	100
corolla	6	47	7.8	15.6
corolla + transgene	9	571	63.4	126.2

[a] Individual females tested.

The *corolla* gene is predicted to encode a 554-amino-acid protein with three internal coiled-coil domains (FlyBase and Coils) (Figure 1C and Supporting Information, Figure S1) (Lupas *et al.* 1991). All four known alleles of *corolla* (shown in Figure 1A) exhibit DNA sequence changes in the third exon of this gene. *corolla*^{1}, *corolla*^{129}, and *corolla*^{166} are the result of mutations that would be predicted to truncate the Corolla protein at amino acids 173, 199, and 188 (see *Materials and Methods*), respectively, while *P{XP}CG8316*^{d01774} is a *P*-element insertion mutant in exon 3. The three EMS-induced alleles behave similarly in all assays tested, and therefore we will discuss *corolla*^{1} exclusively in this article. In addition, based both on studies that we will discuss below and the fact that the meiotic phenotype of *corolla*^{1} homozygotes was similar to *corolla*^{1}*/Df(corolla)* heterozygotes (data not shown), we will propose that *corolla*^{1} is a null allele.

Corolla encodes a SC component and is required for proper SC formation

Given that *corolla* appears to encode a protein with coiled-coil domains—a known conserved domain within components of the CR—and that mutations in *corolla* cause high levels of meiosis I nondisjunction (Collins *et al.* 2012), we speculated that Corolla might be a component of the SC. We generated antibodies to Corolla and performed immunofluorescence assays on ovaries from wild-type females. As shown in Figure 1D, Corolla localizes to the SC in a pattern that closely mimics that of the transverse filament protein C(3)G and the CE protein Cona. In the absence of *corolla*, SC formation is abolished (Figure 1D). This defect in SC formation can be rescued by a transgene bearing a genomic copy of *corolla* (data not shown), confirming that Corolla is essential for SC formation.

corolla mutants exhibit phenotypes consistent with a role in SC formation and function

Proteins involved in forming the structure of the SC tend to display many of the same phenotypes. In general terms, mutations in these genes cause the following: (1) a failure to cluster centromeres in early prophase and to maintain the pairing of homologous centromeres (Takeo *et al.* 2011; Tanneti *et al.* 2011); (2) a reduction in the frequency of programmed DSBs (Mehrotra and McKim 2006); and (3) greatly reduced or abolished meiotic recombination (Page

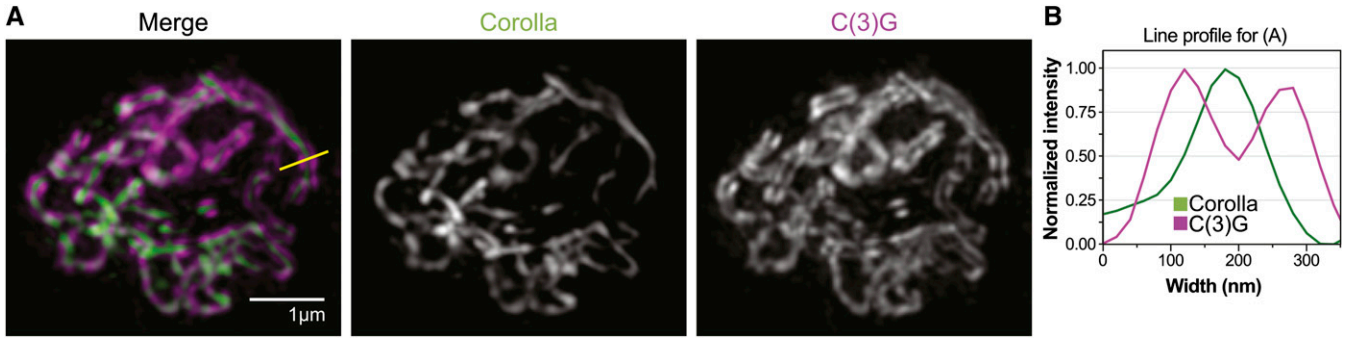

Figure 2 Corolla localizes to the central region of the SC. (A) DeltaVision OMX microscopy of C(3)G (C-terminal domain) (magenta, AF488) and Corolla (green, AF555). Maximum-intensity projections are shown of a few Z slices. See Figure S2B for a representative image of a maximum-intensity projection through an entire pachytene pro-oocyte. (B) Representative line profiles plot the normalized intensity for Corolla (green) and C(3)G (magenta). The line profile in B is from A. Two peaks of C(3)G intensity represent the parallel tracks of C(3)G, and the Corolla peak is positioned clearly between the two C(3)G peaks.

and Hawley 2001; Manheim and McKim 2003; Page *et al.* 2007). As described in detail below, *corolla* mutants also affect each of these processes, consistent with the hypothesis that Corolla functions as an integral component of the SC.

We begin by demonstrating that *corolla* mutants exhibit a severe defect in meiotic centromere clustering. *Drosophila* females have four pairs of homologous chromosomes, which cluster in early prophase within the germarium. The number of centromere clusters is obtained by counting the number of foci observed using an antibody against the *Drosophila* CID protein (CENP-A homolog) (Blower and Karpen 2001). Typically, one or two CID clusters are seen in wild-type oocytes (Takeo *et al.* 2011; Tanneti *et al.* 2011). However, in mutants that are defective in SC formation/maintenance, centromere clustering is abrogated, increasing the number of CID foci to three or four, and often homologous centromeres become unpaired, resulting in the observation of more than four CID foci (Takeo *et al.* 2011).

We measured the extent of both centromere clustering and centromere pairing in *corolla* by determining the percentage of a given genotype that displayed either a decrease in oocytes with one or two CID foci (a centromere clustering defect) or displayed more than four CID foci (a centromere pairing defect).

Since *corolla* is defective in SC formation, it is difficult to distinguish oocyte nuclei from nurse-cell nuclei in early stages of pachytene. Therefore, we chose to analyze oocytes in region 3 of the germarium where the oocyte nucleus is easily identifiable by costaining with Orb, which concentrates in the cytoplasm of the specified oocyte. As shown in Figure 1E and Table S1, the number of oocytes with one or two CID foci decreased from 76.3% observed in wild type to 0% in *corolla*, indicative of a strong defect in centromere clustering. Additionally, although oocytes with more than four foci were never observed in wild-type oocytes, in *corolla* oocytes we found that 21.9% of nuclei scored had more than four CID foci, suggesting that *corolla* mutants are also strongly defective in centromere pairing. These defects in centromere clustering and centromere pairing are comparable to those exhibited by other SC mutants. For example, a *c(3)G* mutant showed a significant reduction in one or two CID foci [80.7% in wild type to 6.3% in *c(3)G*], and 28.1% of region 3 oocyte nuclei had more than four CID foci (Takeo *et al.* 2011).

Previous studies have also shown that SC disruption can lead to reduced DSB formation (Mehrotra and McKim 2006). To assay the number of DSBs, we used a monoclonal antibody recognizing the phosphorylated form of H2AV, called γ-H2AV (Lake *et al.* 2013), and used the cytoplasmic marker Orb to mark the early–mid-pachytene oocyte nuclei in region 3 (Figure 1F). Because the formation and repair of DSBs is a dynamic process, and to determine more accurately the number of DSBs generated in early pachytene, we utilized a DSB repair-defective background (*okra*) to assay the total number of DSBs made (Ghabrial *et al.* 1998; Jang *et al.* 2003; Mehrotra and McKim 2006). As anticipated, we found that *corolla*; *okra* double mutants exhibited a reduced number of γ-H2AV foci (average of 8.3 foci per oocyte, $n = 15$ oocytes), displaying only 37% of the DSBs observed in the *okra* control genotype (average of 22.3 foci per oocyte, $n = 10$ oocytes) (set to 100%) (Table S2). This is similar to the range of reduction seen by Mehrotra and McKim (2006) in the LE mutant *c(2)M* (44.8% of *okra* control) and the TF mutant *c(3)G* (15–21.3% of *okra* control) in the absence of repair. Thus, although Corolla is not essential for DSB formation, like other SC proteins it is required for normal levels of DSB formation. Moreover, the following analysis of recombination shows that Corolla is required to process DSBs into mature crossovers.

The high levels of nondisjunction seen in *corolla* mutants are easily explained by the reduction in meiotic recombination (Figure 1G). While the wild-type control exhibited levels of recombination on the third chromosome similar to previous studies (Manheim and McKim 2003), *corolla* exhibited no recombination throughout most of the euchromatin and exhibited a reduced frequency of recombination in the centromere-proximal interval. These reduced levels of recombination are fully consistent with the high levels of

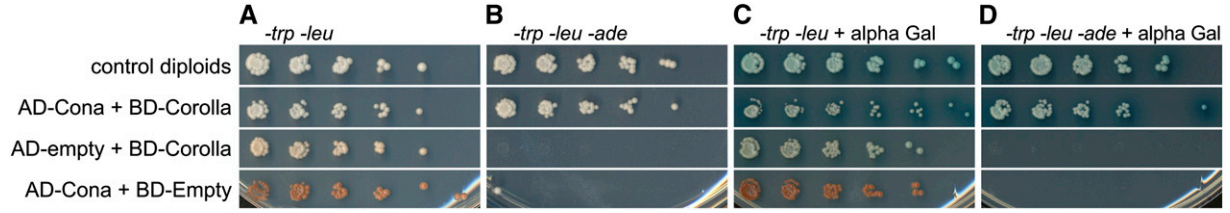

Figure 3 Corolla strongly interacts with Cona by yeast two-hybrid. (A) All diploid strains grow equally well under selection for both the AD and BD plasmids (*–trp–leu*). (B) AD-Cona and BD-Corolla strongly interact on the *ADE2* reporter assay (*–trp–leu–ade*). No interaction was detected with AD-empty and a BD-Corolla construct or between AD-Cona and an empty BD construct. (C) AD-Cona and BD-Corolla strongly interact on the *MEL1* reporter assay (of *–trp–leu* + X-α-Gal). It should be noted that BD-Corolla weakly autoactivates the *MEL1* reporter. (D) AD-Cona and BD-Corolla strongly interact under the most stringent selection of *–trp–leu–ade* + X-α-Gal.

nondisjunction observed in *corolla* mutants. Although the same number of females were tested, fewer progeny were scored in *corolla* ($n = 168$) than in wild type ($n = 1271$) due to a fertility defect of *corolla* mutants (Table 1), which may well be the consequence of chromosome missegregation.

Taken together, these data suggest that, at least as assayed genetically, Corolla acts as an integral member of the SC, such that *corolla* mutants show the same cluster of meiotic defects exhibited by mutants in genes encoding other known SC components.

Corolla localizes to the central region of the synaptonemal complex

To determine the precise location of Corolla within the SC, we performed studies using SIM. First, to ascertain if we could resolve the lateral edge of the SC from the central region, we analyzed by SIM the colocalization of C(3)G and Cona. Using an antibody to the C-terminal globular domain of C(3)G that has been shown by immuno-electron microscopy (EM) to localize at the lateral edges of the TF, abutting the LE (*Anderson et al.* 2005), we were able to resolve two parallel tracks of C(3)G localization. As predicted from preliminary immuno-EM studies used to analyze the location of Cona:: venus overexpressed in wild-type ovaries (Lake and Hawley 2012), Cona localized between the two tracks of the lateral edges of the TF (Figure S2).

We determined the distance between the two C(3)G tracks to be 137 ± 3 nm (Figure S3, A and B). Our data for SC width are slightly greater than the number (109 ± 8 nm) obtained by Carpenter's EM analysis of the *Drosophila* SC (Carpenter 1975). One possible explanation for this discrepancy may be that the C-terminal epitope of C(3)G is buried within the LE. Indeed, the immuno-EM done by Anderson *et al.* (2005) using this antibody shows C(3)G localization that appears within the electron dense LE tracks.

As we were able to resolve the lateral sides of the SC from the central region using SIM, we next determined the localization of Corolla within the SC by costaining wild-type oocytes with antibodies to Corolla and the C-terminal end of C(3)G (Figure 2A, Figure S2B, File S1, and File S2). The immunofluorescence signal for Corolla was similar to that for Cona, in that the Corolla signal ran between the two tracks of C(3)G. When a line profile was drawn perpendicular to a parallel track of C(3)G, two peaks of the C(3)G signal are clearly visible and only one peak of Corolla is present in between the two C(3)G peaks (Figure 2B). While in the vast majority of cases (33/34), the Corolla signal appeared as a single peak in a line profile, Corolla appeared as a double peak in 1/34 cases. The significance of this one unusual profile, if any, is currently not understood. In conclusion, SIM technology enabled us to localize Corolla within the SC; specifically, Corolla localizes to the CR of the SC.

Corolla interacts with Cona by yeast two-hybrid

Since SIM analysis virtually always identified Corolla as a single track running between the lateral sides of the SC—a pattern very similar to Cona—we wanted to determine whether Corolla and Cona physically interact. To test this, we performed yeast two-hybrid analysis (Figure 3). We assayed BD-Corolla/AD-Cona interaction on the *ADE2* reporter, as well as in the *MEL1* assay. Diploids containing BD-Corolla and AD-Cona were able to grow on media lacking adenine and exhibited a deep blue color indistinguishable from the diploid positive control in the presence of X-α-gal, thus illustrating that Cona-Corolla strongly interact. This provides the first evidence of a physical linkage between any two *Drosophila* inner-SC proteins. Corolla was named for this interaction with Cona, whose full name is Corona, as Corolla is the Latin diminutive of Corona.

Corolla may self-associate, but does not appear to localize to the chromosome axes in the absence of C(3)G

Since Corolla contains coiled-coil domains and physically interacts with Cona, we next addressed whether Corolla could associate with the chromosomes in the absence of the TF protein C(3)G. Whole-mount immunofluorescence imaging using standard deconvolution microscopy demonstrated that the Corolla signal persisted in early pachytene nuclei (region 2A) in the absence of the TF protein C(3)G, although the signal appeared more diffuse and less ribbon-like than the wild type (Figure 4).

The Corolla staining observed in Figure 4B was unanticipated since previous EM analysis of *c(3)G* mutants did not reveal any SC structure (Smith and King 1968). In an attempt to resolve this issue, we performed immunofluorescence analysis

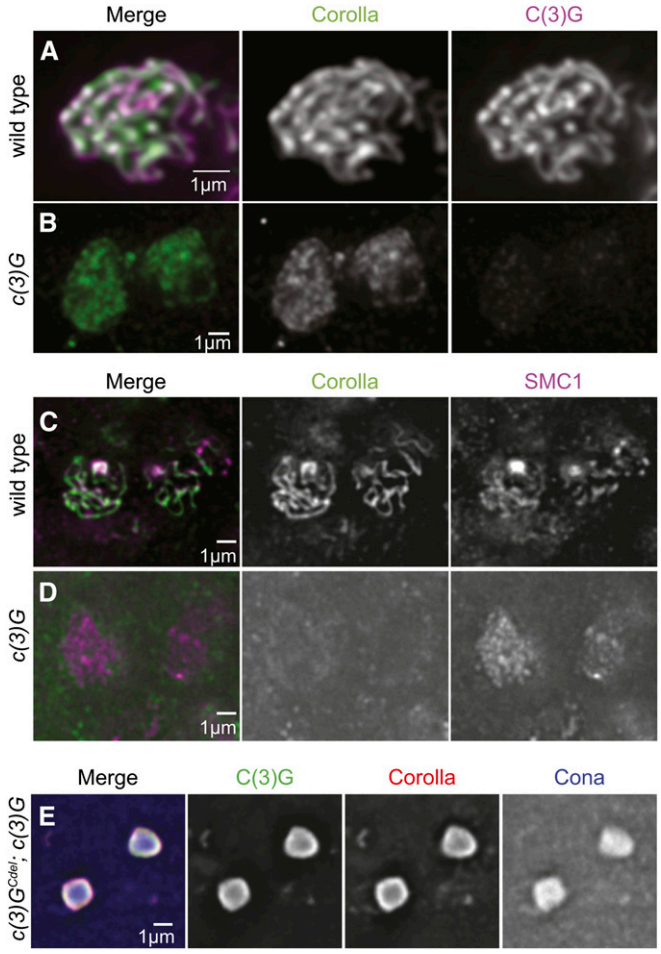

Figure 4 Corolla localization in *c(3)G* mutants. (A and B) Pachytene pro-oocyte nuclei from wild type and a *c(3)G* mutant showing the localization of Corolla (green) and C(3)G (magenta) in whole-mount tissue. (A) C(3)G and Corolla appear as clear ribbons of SC by standard deconvolution imaging in wild-type oocytes. (B) Corolla signal persists in early pachytene nuclei of *c(3)G* mutants as a diffuse ribbon-like structure. (C and D) Pachytene nuclei from wild type and a *c(3)G* mutant showing localization of Corolla (green) and SMC1 (magenta) in chromosome spread preparations. (C) Corolla colocalizes with SMC1 in wild-type oocytes. (D) Corolla staining is not preserved in chromosome spreads of a *c(3)G* mutant. (E) DeltaVision microscopy of C(3)G (green) identified by anti-Flag antibody, Corolla (red), and Cona (blue) in early–mid-pachytene oocytes from *nanos-GAL4::VP16/yw*; *UASp-c(3)G$^{Cdel\text{-}Flag}$/+*; *c(3)G^{68}*. Corolla localizes to polycomplexes when C(3)G is unable to associate with the LEs. Maximum-intensity projections are shown of a few Z slices in A–D, and a single Z slice is shown in E.

on chromosome spreads of wild-type and *c(3)G* mutant oocytes immunostained with Corolla and the cohesin component SMC1 to visualize the lateral elements of the SC (Figure 4, C and D). Previous studies have shown that loading of the cohesin components SMC1 and SMC3 is not affected in the absence of *c(3)G* (Khetani and Bickel 2007). Chromosome spread preparation of ovaries, in which soluble components not attached to chromatin are removed (Khetani and Bickel 2007), enabled us to determine whether Corolla localizes to meiotic chromosomes in the absence of *c(3)G*. In 40 partially intact germaria, we did not detect any chromatin-associated Corolla (one example shown in Figure 4D), suggesting that the structure of Corolla seen in whole-mount *c(3)G* oocytes does not appear to associate with chromosomes. We speculate that Corolla may be self-assembling via the coiled-coil domains; however, these complexes do not associate with the LEs. Thus, based on these observations and those described above, Corolla and C(3)G appear mutually dependent with regard to localization to meiotic chromosomes.

In addition, we also analyzed Corolla's localization in oocytes expressing a mutation of *c(3)G* that lacks the C-terminal globular domain of the C(3)G protein (Jeffress *et al.* 2007). In this mutant, C(3)G cannot attach to the LEs, and therefore instead of assembling along the chromosomes, the proteins composing the central region of the SC are assembled into aggregates called polycomplexes. In the absence of C(3)G association with the LEs, we find that Corolla, like Cona, assembles into polycomplexes (Figure 4E). This result further supports the findings that Corolla is a CR component of the SC and does not associate with the LEs in the absence of C(3)G.

Discussion

This article both describes the utility of SIM for the analysis of SC in wild-type and mutant *Drosophila* oocytes and reports the identification of Corolla, a new component of the central region of the *Drosophila* SC. We have further shown that Corolla physically interacts with another central region protein, Cona. We previously presented preliminary immuno-EM data suggesting that Cona localizes to the edges of the CE (Page *et al.* 2008; Lake and Hawley 2012). The discovery of Corolla raises the number of central region proteins identified in *Drosophila* to three [Corolla, Cona, and C(3)G], each of which is dependent on the other two for establishing the SC. We propose that, while the binding of these three proteins to the paired homologs is mediated by the attachment of the C terminus of C(3)G to the LE, both Cona and Corolla are required to stabilize the interactions between oppositely oriented C(3)G proteins (transverse filament proteins), which are required to form nascent complexes that can be attached to the LE. In the absence of the C terminus of C(3)G, the three known central region proteins (and presumably others) can form polycomplexes that fail to attach to the chromosomes.

Perhaps because these three proteins are so functionally interdependent, the phenotypes of *corolla* mutants are virtually identical to those of *cona* and *c(3)G* mutants (Page and Hawley 2001; Mehrotra and McKim 2006; Page *et al.* 2008; Takeo *et al.* 2011). These phenotypes include a reduction in the number of meiotic DSBs, a near elimination of meiotic recombination (and a concomitant increase in meiotic nondisjunction), and a loss of centromere clustering. We imagine that the similarity of meiotic defects exhibited by all three mutants reflects the fact that these act as part of a functional identity, such that each component is left functionless without the other two.

Anderson *et al.* (2005) used immuno-EM to show that C(3)G spanned the distance between the LEs and the middle of the CE, and Öllinger *et al.* (2005) has shown that

expression of the rat TF protein, SCP1, alone in cultured cells can facilitate the assembly of polycomplex-like structures. Why then does the *Drosophila* oocyte require additional proteins such as Cona and Corolla to build an SC, and what specifically is the function of Corolla? Perhaps the answer lies in (1) Cona's position in the central region, where it could act to stabilize the antiparallel interactions between C(3)G homodimers emanating from opposite LEs; (2) Corolla's ability to physically interact with Cona; and (3) a hypothetical interaction between the coiled-coil domains of Corolla and C(3)G.

Although *corolla* encodes what appears to be a novel protein, we have identified three short regions of amino acid homology between Corolla and the *C. elegans* SYP-4 protein (Figure S4). SYP-4 is one of the *C. elegans* TF proteins, which, like Corolla, localizes within the central region and reaches out toward the lateral elements (Schild-Prüfert *et al.* 2011). SYP-4 is a slightly larger protein than Corolla (605 *vs.* 554 amino acids) and is not known to have any identifiable structural motifs (other than three predicted coiled-coils that span amino acids 115–410) or homology to any known protein in any organism (Smolikov *et al.* 2009). Moreover, *syp-4* mutants have no detectable SC structure present by transmission electron microscopy (Smolikov *et al.* 2009). This is similar to corolla mutants, which fail to show a discernible SC structure when assayed by SIM (data not shown).

One common feature of SC proteins (particularly those of the CR) is the presence of protein domains that are predicted to be coiled-coils. Coiled-coil domains are known to promote oligomerization and often interact with other proteins that contain coiled-coils (Newman *et al.* 2000). In mice, the CR is known to contain five proteins, four of which are predicted to have coiled-coil domains (SYCP1, SYCE1, SYCE2, and SYCE3) and one (TEX12) that does not contain a coiled-coil domain (Fraune *et al.* 2012b). In *C. elegans*, all four known CR proteins (SYP-1, SYP-2, SYP-3, and SYP-4) have coiled-coil domains (Smolikov *et al.* 2009; Schild-Prüfert *et al.* 2011). In *Drosophila*, although C(3)G has multiple coiled-coil domains (Page and Hawley 2001; Jeffress *et al.* 2007), Cona is not predicted to possess any (Page *et al.* 2008). Corolla, as shown in Figure S1, is predicted by the COILS program to contain multiple coiled-coil domains.

In addition to coiled-coil domains, another hallmark of TF proteins is that the coiled-coil domains are flanked by globular domains (Zickler and Kleckner 1999; Page and Hawley 2004; de Boer and Heyting 2006). Using the Eukaryotic Linear Motif (ELM) resource (Puntervoll *et al.* 2003), we analyzed the protein sequence of Corolla in search of globular domains that flanked the predicted coiled-coil domains. ELM analysis identified that Corolla, like other TF proteins, contains globular domains that flank the predicted coiled-coil domains that were identified by COILS (Figure S1 and Figure S4B). Taken together, the short regions of possible homology, the similar size with the presence of multiple coiled-coil regions that are flanked by globular domains, and the similar localization (by SIM for Corolla and by immuno-EM for SYP-4), it seems at least possible that Corolla could be the fly ortholog of the TF protein SYP-4.

Acknowledgments

We thank Kim McKim, Claudio Sunkel, and Sharon Bickel for antibodies; Kendra Walton for NGS sample preparation assistance; Jim Vallandingham for NGS data analysis assistance; Hua Li for bioinformatics advice; Angela Miller for graphics; and Hawley Laboratory members for helpful advice on the manuscript. RSH is supported by the Stowers Institute for Medical Research and is an American Cancer Society Research Professor supported by the award RP-05-086-06 DDC.

Literature Cited

Alsheimer, M., A. Baier, S. Schramm, W. Schütz, and R. Benavente, 2010 Synaptonemal complex protein SYCP3 exists in two isoforms showing different conservation in mammalian evolution. Cytogenet. Genome Res. 128: 162–168.

Anderson, L. K., S. M. Royer, S. L. Page, K. S. McKim, A. Lai *et al.*, 2005 Juxtaposition of C(2)M and the transverse filament protein C(3)G within the central region of Drosophila synaptonemal complex. Proc. Natl. Acad. Sci. USA 102: 4482–4487.

Blower, M. D., and G. Karpen, 2001 The role of Drosophila CID in kinetochore formation, cell-cycle progression and heterochromatin interactions. Nat. Cell Biol. 3: 730–739.

Blumenstiel, J. P., A. C. Noll, J. A. Griffiths, A. G. Perera, K. N. Walton *et al.*, 2009 Identification of EMS-induced mutations in *Drosophila melanogaster* by whole-genome sequencing. Genetics 182: 25–32.

Carpenter, A. T., 1975 Electron microscopy of meiosis in Drosophila melanogaster females: II. The recombination nodule: A recombination-associated structure at pachytene? Proc. Natl. Acad. Sci. USA 72: 3186–3189.

Cingolani, P., A. Platts, L. L. Wang, M. Coon, T. Nguyen *et al.*, 2012 A program for annotating and predicting the effects of single nucleotide polymorphisms, SnpEff: SNPs in the genome of *Drosophila melanogaster* strain *w1118*; *iso-2;iso-3*. Fly (Austin) 6: 80–92.

Colaiácovo, M. P., A. J. MacQueen, E. Martinez-Perez, K. McDonald, A. Adamo *et al.*, 2003 Synaptonemal complex assembly in C. elegans is dispensable for loading strand-exchange proteins but critical for proper completion of recombination. Dev. Cell 5: 463–474.

Collins, K. A., J. G. Callicoat, C. M. Lake, C. M. McClurken, K. P. Kohl *et al.*, 2012 A germline clone screen on the X chromosome reveals novel meiotic mutants in *Drosophila melanogaster*. G3 2: 1369–1377.

de Boer, E., and C. Heyting, 2006 The diverse roles of transverse filaments of synaptonemal complexes in meiosis. Chromosoma 115: 220–234.

DePristo, M. A., E. Banks, R. Poplin, K. V. Garimella, J. R. Maguire *et al.*, 2011 A framework for variation discovery and genotyping using next-generation DNA sequencing data. Nat. Genet. 43: 491–498.

Fraune, J., M. Alsheimer, J.-N. Volff, K. Busch, S. Fraune *et al.*, 2012a Hydra meiosis reveals unexpected conservation of structural synaptonemal complex proteins across metazoans. Proc. Natl. Acad. Sci. USA 109: 16588–16593.

Fraune, J., S. Schramm, M. Alsheimer, and R. Benavente, 2012b The mammalian synaptonemal complex: protein com-

ponents, assembly and role in meiotic recombination. Exp. Cell Res. 318: 1340–1346.
Ghabrial, A., R. P. Ray, and T. Schüpbach, 1998 okra and spindle-B encode components of the RAD52 DNA repair pathway and affect meiosis and patterning in Drosophila oogenesis. Genes Dev. 12: 2711–2723.
Gloor, G. B., C. R. Preston, D. M. Johnson-Schlitz, N. A. Nassif, R. W. Phillis *et al.*, 1993 Type I repressors of P element mobility. Genetics 135: 81–95.
Hawley, R. S., H. Irick, A. E. Zitron, D. A. Haddox, A. Lohe *et al.*, 1992 There are two mechanisms of achiasmate segregation in Drosophila females, one of which requires heterochromatic homology. Dev. Genet. 13: 440–467.
James, P., J. Halladay, and E. A. Craig, 1996 Genomic libraries and a host strain designed for highly efficient two-hybrid selection in yeast. Genetics 144: 1425–1436.
Jang, J. K., D. E. Sherizen, R. Bhagat, E. A. Manheim, and K. S. McKim, 2003 Relationship of DNA double-strand breaks to synapsis in *Drosophila*. J. Cell Sci. 116: 3069–3077.
Jeffress, J. K., S. L. Page, S. M. Royer, E. D. Belden, J. P. Blumenstiel *et al.*, 2007 The formation of the central element of the synaptonemal complex may occur by multiple mechanisms: the roles of the N- and C-terminal domains of the Drosophila C(3)G protein in mediating synapsis and recombination. Genetics 177: 2445–2456.
Joyce, E. F., and K. S. McKim, 2009 Drosophila PCH2 is required for a pachytene checkpoint that monitors double-strand-break-independent events leading to meiotic crossover formation. Genetics 181: 39–51.
Khetani, R. S., and S. E. Bickel, 2007 Regulation of meiotic cohesion and chromosome core morphogenesis during pachytene in Drosophila oocytes. J. Cell Sci. 120: 3123–3137.
Lake, C. M., and R. S. Hawley, 2012 The molecular control of meiotic chromosomal behavior: events in early meiotic prophase in Drosophila oocytes. Annu. Rev. Physiol. 74: 425–451.
Lake, C. M., J. K. Holsclaw, S. P. Bellendir, J. Sekelsky,, and R. S. Hawley, 2013 The development of a monoclonal antibody recognizing the *Drosophila melanogaster* phosphorylated histone H2A variant (γ-H2AV). G3 3: 1539–1543.
Lammers, J. H., H. H. Offenberg, M. van Aalderen, A. C. Vink, A. J. Dietrich *et al.*, 1994 The gene encoding a major component of the lateral elements of synaptonemal complexes of the rat is related to X-linked lymphocyte-regulated genes. Mol. Cell. Biol. 14: 1137–1146.
Li, H., and R. Durbin, 2009 Fast and accurate short read alignment with Burrows–Wheeler transform. Bioinformatics 25: 1754–1760.
Lupas, A., M. Van Dyke, and J. Stock, 1991 Predicting coiled coils from protein sequences. Science 252: 1162–1164.
MacQueen, A. J., M. P. Colaiácovo, K. McDonald, and A. M. Villeneuve, 2002 Synapsis-dependent and -independent mechanisms stabilize homolog pairing during meiotic prophase in C. elegans. Genes Dev. 16: 2428–2442.
Manheim, E. A., and K. S. McKim, 2003 The synaptonemal complex component C(2)M regulates meiotic crossing over in Drosophila. Curr. Biol. 13: 276–285.
Markstein, M., C. Pitsouli, C. Villalta, S. E. Celniker, and N. Perrimon, 2008 Exploiting position effects and the gypsy retrovirus insulator to engineer precisely expressed transgenes. Nat. Genet. 40: 476–483.
Martins, T., A. F. Maia, S. Steffensen, and C. E. Sunkel, 2009 Sgt1, a co-chaperone of Hsp90 stabilizes Polo and is required for centrosome organization. EMBO J. 28: 234–247.
McKenna, A., M. Hanna, E. Banks, A. Sivachenko, K. Cibulskis *et al.*, 2010 The Genome Analysis Toolkit: A MapReduce framework for analyzing next-generation DNA sequencing data. Genome Res. 20: 1297–1303.
Mehrotra, S., and K. S. McKim, 2006 Temporal analysis of meiotic DNA double-strand break formation and repair in Drosophila females. PLoS Genet. 2: e200.
Newman, J. R. S., E. Wolf, and P. S. Kim, 2000 A computationally directed screen identifying interacting coiled coils from Saccharomyces cerevisiae. Proc. Natl. Acad. Sci. USA 97: 13203–13208.
Öllinger, R., M. Alsheimer, and R. Benavente, 2005 Mammalian protein SCP1 forms synaptonemal complex-like structures in the absence of meiotic chromosomes. Mol. Biol. Cell 16: 212–217.
Page, S. L., and R. S. Hawley, 2001 c(3)G encodes a Drosophila synaptonemal complex protein. Genes Dev. 15: 3130–3143.
Page, S. L., and R. S. Hawley, 2004 The genetics and molecular biology of the synaptonemal complex. Annu. Rev. Cell Dev. Biol. 20: 525–558.
Page, S., R. J. Nielsen, K. Teeter, C. M. Lake, S. Ong *et al.*, 2007 A germline clone screen for meiotic mutants in *Drosophila melanogaster*. Fly (Austin) 1: 172–181.
Page, S. L., R. S. Khetani, C. M. Lake, R. J. Nielsen, J. K. Jeffress *et al.*, 2008 *corona* is required for higher-order assembly of transverse filaments into full-length synaptonemal complex in Drosophila oocytes. PLoS Genet. 4: e1000194.
Puntervoll, P., R. Linding, C. Gemünd, S. Chabanis-Davidson, M. Mattingsdal *et al.*, 2003 ELM server: a new resource for investigating short functional sites in modular eukaryotic proteins. Nucleic Acids Res. 31: 3625–3630.
Schild-Prüfert, K., T. T. Saito, S. Smolikov, Y. Gu, M. Hincapie *et al.*, 2011 Organization of the synaptonemal complex during meiosis in *Caenorhabditis elegans*. Genetics 189: 411–421.
Smith, P. A., and R. C. King, 1968 Genetic control of synaptonemal complexes in *Drosophila melanogaster*. Genetics 60: 335–351.
Smolikov, S., A. Eizinger, K. Schild-Prufert, A. Hurlburt, K. McDonald *et al.*, 2007 SYP-3 restricts synaptonemal complex assembly to bridge paired chromosome axes during meiosis in *Caenorhabditis elegans*. Genetics 176: 2015–2025.
Smolikov, S., K. Schild-Prüfert, and M. P. Colaiácovo, 2009 A yeast two-hybrid screen for SYP-3 interactors identifies SYP-4, a component required for synaptonemal complex assembly and chiasma formation in *Caenorhabditis elegans* meiosis. PLoS Genet. 5: e1000669.
Takeo, S., and M. C. Lake, E. Morais-de-Sá, C. E. Sunkel, and R. S. Hawley, 2011 Synaptonemal complex-dependent centromeric clustering and the initiation of synapsis in Drosophila oocytes. Curr. Biol. 21: 1845–1851.
Tanneti, Nikhila S., K. Landy, Eric F. Joyce, and Kim S. McKim, 2011 A pathway for synapsis initiation during zygotene in *Drosophila* oocytes. Curr. Biol. 21: 1852–1857.
Thevenaz, P., U. E. Ruttimann, and M. Unser, 1998 A pyramid approach to subpixel registration based on intensity. IEEE Trans. Image Process. 7: 27–41.
Wade Harper, J., G. R. Adami, N. Wei, K. Keyomarsi, and S. J. Elledge, 1993 The p21 Cdk-interacting protein Cip1 is a potent inhibitor of G1 cyclin-dependent kinases. Cell 75: 805–816.
Watts, F. Z., and E. Hoffmann, 2011 SUMO meets meiosis: an encounter at the synaptonemal complex. BioEssays 33: 529–537.
Webber, H. A., L. Howard, and S. E. Bickel, 2004 The cohesion protein ORD is required for homologue bias during meiotic recombination. J. Cell Biol. 164: 819–829.
Yan, R., and B. D. McKee, 2013 The cohesion protein SOLO associates with SMC1 and is required for synapsis, recombination, homolog bias and cohesion and pairing of centromeres in Drosophila meiosis. PLoS Genet. 9: e1003637.
Zickler, D., and N. Kleckner, 1999 Meiotic chromosomes: integrating structure and function. Annu. Rev. Genet. 33: 603–754.
Zitron, A. E., and R. S. Hawley, 1989 The genetic analysis of distributive segregation in *Drosophila melanogaster*. I. Isolation and characterization of aberrant X segregation (Axs), a mutation defective in chromosome partner choice. Genetics 122: 801–821.

Communicating editor: M. P. Colaiácovo

GENETICS

Supporting Information
http://www.genetics.org/lookup/suppl/doi:10.1534/genetics.114.165290/-/DC1

Corolla Is a Novel Protein That Contributes to the Architecture of the Synaptonemal Complex of *Drosophila*

Kimberly A. Collins, Jay R. Unruh, Brian D. Slaughter, Zulin Yu, Cathleen M. Lake, Rachel J. Nielsen, Kimberly S. Box, Danny E. Miller, Justin P. Blumenstiel, Anoja G. Perera, Kathryn E. Malanowski, and R. Scott Hawley

DOI: 10.1534/genetics.114.165290

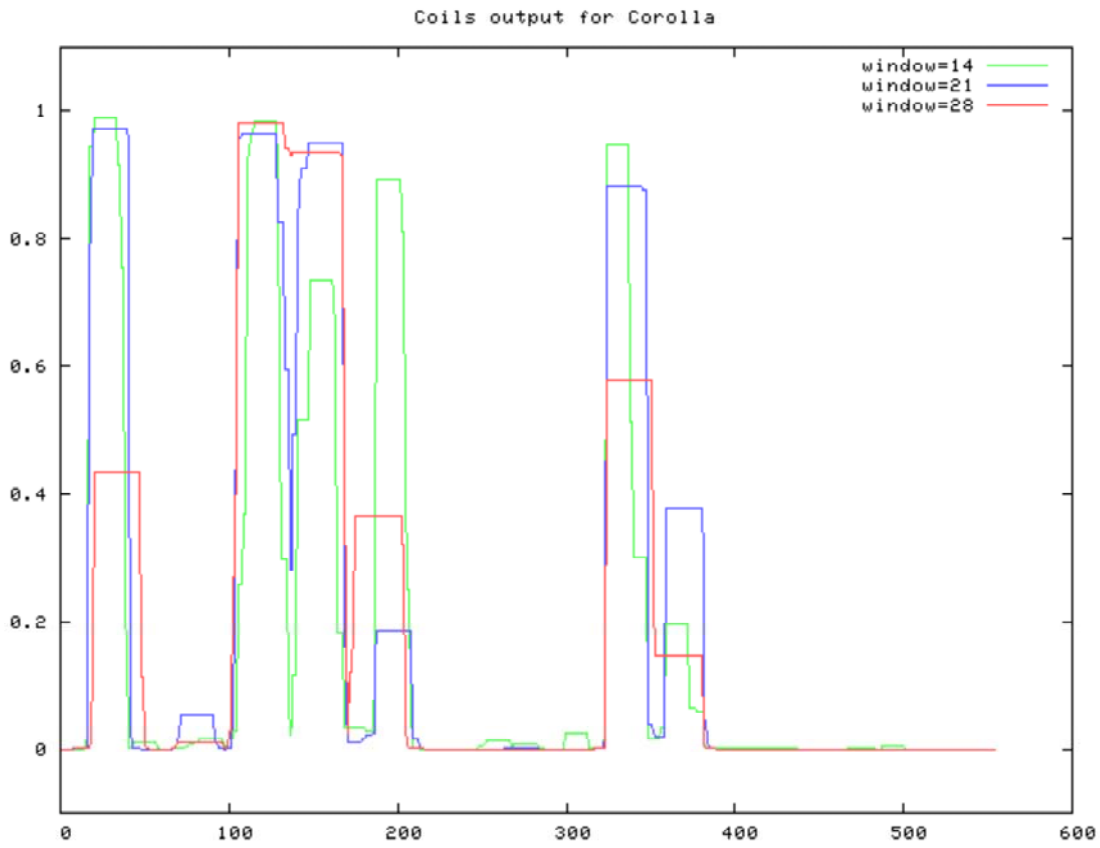

Figure S1 Coiled-coil prediction of Corolla by the COILS program. Corolla is predicted to contain three coiled-coil regions based on the COILS program (Lupas *et al.* 1991). These coiled-coil domains span the first two-thirds of the protein. Of note, the Eukaryotic Linear Motif (ELM) program (http://elm.eu.org/) identified only one coiled-coil domain in Corolla (aa 105–135) (Dinkel *et al.* 2014).

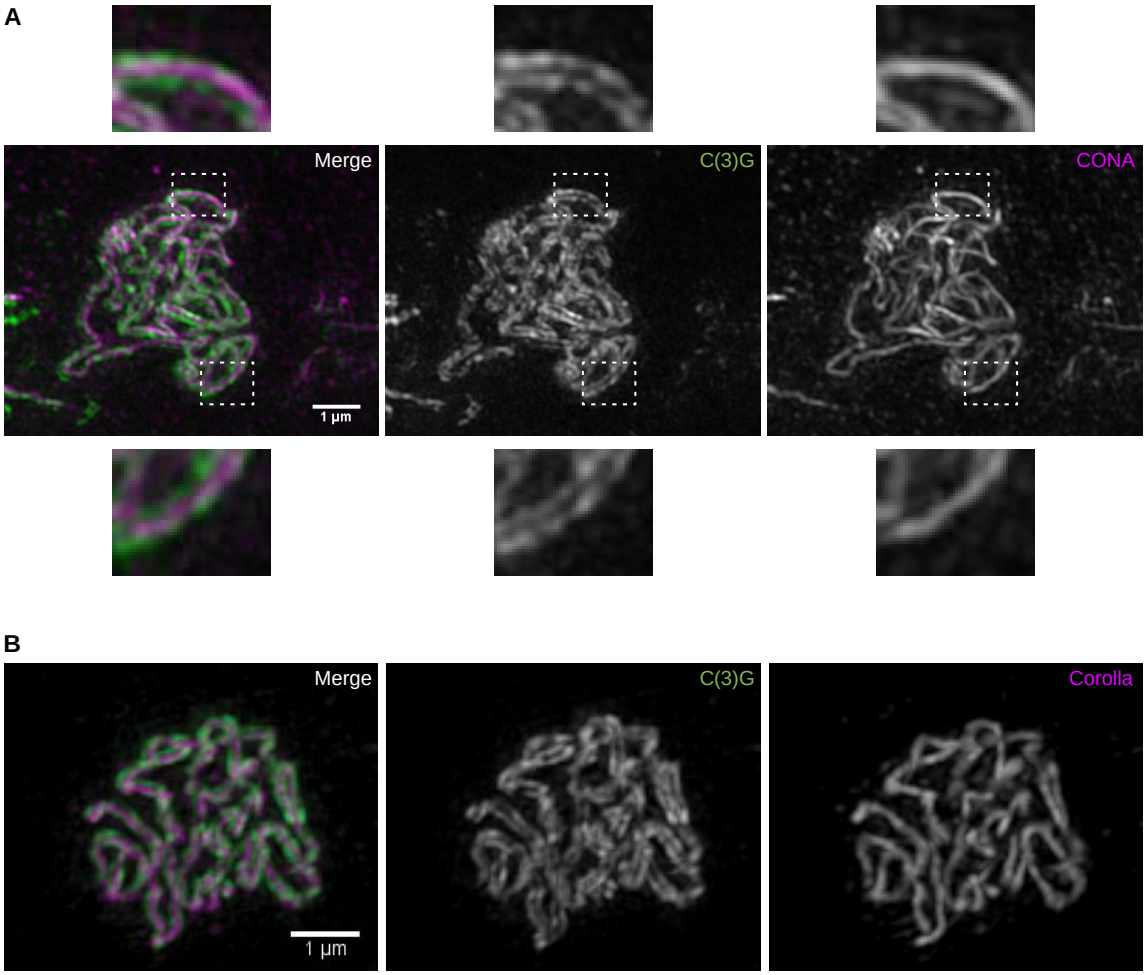

Figure S2 SIM imaging of a wild-type pachytene oocyte for Cona, C(3)G and Corolla. (A) DeltaVision OMX microscopy of C(3)G (C-terminal domain) (green, AF488) and Cona (magenta, AF555) in a wild-type pachytene oocyte. Maximum-intensity projection of Z-series though an entire pro-oocyte is shown. Two regions outlined with a dashed box are magnified above and below the image to show that Cona is clearly positioned between the two C(3)G tracks. **(B)** DeltaVision OMX microscopy of C(3)G (C-terminal domain) (green, AF488) and Corolla (magenta, AF555) in a wild-type pachytene oocyte. Maximum-intensity projection of Z-series though an entire pro-oocyte is shown.

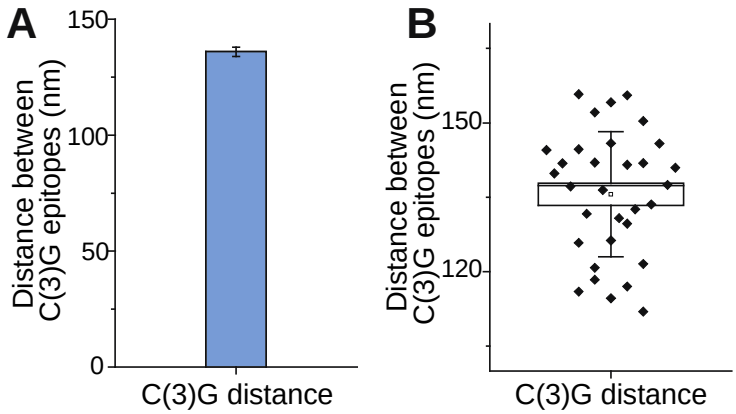

Figure S3 Measurements of the width of the SC by SIM. (A–B) Measurement of the width between C-terminal epitopes of C(3)G. In areas where the SC remained in the same *x-y* plane for an extended period, a line profile was generated and fit to two Gaussians. Error bar indicated the standard error in the mean. **(B)** A box and whisker plot showing the distance between C(3)G epitopes. The small box represents the standard error, the remaining line represents the median, and the whiskers represent standard deviation.

Figure S4 Alignment of protein sequence and predicted secondary structure of Corolla with SYP-4. (A) Clustal alignment of Corolla with SYP-4. *C. elegans* SYP-4 (http://www.ncbi.nlm.nih.gov/protein/CCD72468.1) was aligned to Corolla using Clustal Omega (SIEVERS *et al.* 2011). Three regions of potential homology were detected: region 1, from Corolla amino acids 83 to 95 (69% similarity, 38% identity); region 2, from amino acids 260 to 306 (28% similarity, 23% identity); and region 3, from amino acids 322 to 365 (43% similarity, 34% identity). Hash marks (#) denote removed sequence for ease of viewing the conserved regions and dashes (–) indicate gaps in alignment. Of these three similar regions, only region 3 falls within a predicted coiled-coil region of Corolla (Figure S1). **(B)** ELM analysis (http://elm.eu.org/) of Corolla (FBgn0030852), *C. elegans* SYP-4 (Accession CCD72468), Drosophila TF protein C(3)G (FBgn0000246) and *S. cerevisiae* TF protein Zip1 (Accession AAA35239) showing only the predicted coiled-coil domains, globular domains, low-complexity regions and disordered regions. Note that using the ELM resource, only one coiled-coil region was identified for Corolla and SYP-4, whereas COILS program identified three stretches of coiled-coil regions for both Corolla (Figure S1) and SYP-4 (Smolikov *et al*. 2009). The three coiled-coil stretches identified by COILS for Corolla are between amino acids 17 and 380. For comparison of the coiled-coil domains and flanking globular domains found in other TF proteins, Drosophila C(3)G and *S.cerevisiae* Zip1 are shown. Numbers above vertical lines correspond to amino acid number for each protein. Number at right-hand side corresponds to the total number of amino acids for each protein.

Files S1-S2

Available for download as .mov files at http://www.genetics.org/lookup/suppl/doi:10.1534/genetics.114.165290/-/DC1

File S1 Movie moves through Z slices of a representative nucleus with Corolla in magenta and C(3)G (C-terminal domain) in green as acquired on OMX Blaze microscope.

File S2 Corolla is continuous along the length of the SC. Movie shows rotation in X and Y of a representative nucleus with Corolla in magenta and C(3)G in green as acquired on OMX Blaze microscope.

Table S1 Quantification of the centromere clustering defect in *corolla* mutants.

Genotype	Number of CID foci (%)						*n*	Average ± SD
	1	**2**	**3**	**4**	**5**	**6**		
wild type	16 (42.1)	13 (34.2)	9 (23.7)	0 (0)	0 (0)	0 (0)	38	1.80 ± 0.80
corolla	0 (0)	0 (0)	11 (34.4)	14 (43.8)	4 (12.5)	3 (9.4)	32	3.97 ± 0.93

The number of oocytes in region 3 of the germarium with a given number of CID foci are shown, followed in parentheses by the frequency that a given number of CID foci are seen in a genotype.

Table S2 Frequency of γ-H2AV foci in *corolla* as assayed in the DSB repair-deficient mutant *okra*

Genotype	Average number of foci per Region 3 oocyte	Standard deviation	% of control	Total oocytes analyzed
okra	22.3	1.9	100	10
corolla; *okra*	8.3	2.0	37	15